

NATIVE LEAD AT BROKEN HILL, NEW SOUTH WALES, AUSTRALIA

PAUL F. CARR[§]

School of Earth and Environmental Sciences, University of Wollongong, Wollongong, New South Wales 2522, Australia

BRUCE SELLECK

Department of Geology, Colgate University, Hamilton, New York 13346, USA

MICHAEL STOTT

PO Box 41, Stoneville, Western Australia 6081, Australia

PENNY WILLIAMSON

School of Earth and Environmental Sciences, University of Wollongong, Wollongong, New South Wales 2522, Australia

ABSTRACT

Native lead, a rare mineral, occurs in a late-stage vein in the world's largest lead – zinc – silver deposit, at Broken Hill, Australia. The lead-bearing vein consists mainly of laumontite, quartz, biotite and muscovite, together with minor amounts of lead, galena, sphalerite, molybdenite, and rare allanite-(Ce). Three types of fluid inclusions have been identified: two-phase brine inclusions lacking daughter crystals, brine inclusions “packed” with daughter crystals, and vapor-only inclusions. These fluid inclusions, together with stability data for coexisting minerals, indicate that the native lead formed by precipitation from low-temperature (270–300°C) brines in a near-surface, low-pressure environment. The $^{207}\text{Pb}/^{204}\text{Pb}$ value for the native lead differs significantly from the values for galena and amazonitic orthoclase from the Broken Hill orebody, but overlap the array defined by galena in Cambrian epithermal deposits in the region.

Keywords: native lead, laumontite, fluid inclusions, Broken Hill, New South Wales, Australia.

SOMMAIRE

Le plomb natif, minéral rare, a été trouvé dans une veine tardive à Broken Hill, en Australie, site du plus gros gisement de plomb – zinc – argent au monde. La veine porteuse de plomb contient surtout laumontite, quartz, biotite et muscovite, avec comme accessoires plomb, galène, sphalérite, molybdénite, et allanite-(Ce) plutôt rare. Trois types d'inclusions fluides ont été identifiées: inclusions de saumure à deux phases, dépourvues de cristaux dérivés, des inclusions de saumure “surpeuplées” de cristaux dérivés, et des inclusions ne contenant qu'une phase vapeur. D'après les inclusions fluides, interprétées en fonction des données sur la stabilité des minéraux coexistants, le plomb natif aurait été déposé à partir des saumures à faible température (270–300°C) dans un milieu de faible pression près de la surface. La valeur de $^{207}\text{Pb}/^{204}\text{Pb}$ de ce plomb natif se distingue des valeurs pour la galène et l'orthose amazonitique dans les gisements de Broken Hill, mais rejoint le groupe de valeurs mesurées pour la galène des gisements épithermaux cambriens dans la région.

Traduit par la Rédaction

Mots-clés: plomb natif, laumontite, inclusions fluides, Broken Hill, Nouveau Pays de Galle, Australie.

[§] E-mail address: pcarr@uow.edu.au

INTRODUCTION

The world's largest lead – zinc – silver deposit, at Broken Hill, western New South Wales, in Australia, has produced 200 Mt of ore containing approximately 21 Mt of lead and 19 Mt of zinc, but both metals occur in combined forms, particularly as the sulfides galena and sphalerite. Ironically, the deposit is sulfur-poor (Plimer 1999, 2006), and even with the massive amounts of available lead and zinc and the very wide range of physical and chemical conditions that have affected the Broken Hill lode throughout its geological history, unequivocal occurrences of naturally produced elemental lead or zinc have not been recorded (Birch 1999). Documented occurrences of anthropogenically produced lead include masses up to 15 cm across formed by reduction of galena and cerussite during the mine fires in the late nineteenth and early twentieth centuries (Birch *et al.* 1982, Birch 1999), and small amounts formed by explosive blasting of lead ore during mining (Ian Plimer, pers. commun., 2005). Native zinc has never been reported from Broken Hill.

The only location in the world where significant amounts of native lead have been recovered is Långban, Sweden (Nysten *et al.* 2000), although it also occurs in the famous Franklin, New Jersey, deposits (Dunn 1995), and it has been recorded at several other locations, including Laurium, Greece, where interaction between seawater and ancient metallurgical slags have produced a wide range of rare species including lead (Jaxel & Gelaude 1986). In the current paper, we describe a new occurrence of native lead at Broken Hill, with the aim of determining the conditions required for the formation of this rare mineral.

GEOLOGICAL SETTING

The Broken Hill orebody of the Curnamona Craton is hosted by the intensely metamorphosed (granulite and upper amphibolite facies) and deformed Paleoproterozoic Broken Hill Group, which constitutes one of the six major lithological subdivisions of the Willyama Supergroup (Willis *et al.* 1983). Four major events of deformation and metamorphism overprinted by widespread retrogression are recognized (Wilson & Powell 2001). The Broken Hill Group comprises a metamorphosed sequence of intercalated pelite, psammite, felsic and mafic volcanic rocks, and minor calc-silicate and iron-rich horizons. Quartzofeldspathic gneisses probably originated from felsic volcanic rocks and associated granitic sills, whereas basaltic flows and associated doleritic intrusions were metamorphosed to amphibolites (Stevens 1999). The famous orebody consists of six discrete, parallel and stratigraphically controlled masses of sulfide-rich rocks comprising four zinc lodes (designated No. 1 Lens, A Lode, B Lode and C Lode) and two lead lodes (designated No. 2 lens

and No. 3 lens). Several of these lodes can be further subdivided into smaller lenses, including the Western A lode. The orebody is intimately associated with rocks bearing manganese-rich garnet formed by reaction of pelites with manganese released during deformation and metamorphism (Plimer 2006).

In addition to these stratigraphically controlled masses of sulfide-rich rocks, small, epithermal deposits are also developed throughout the Broken Hill region, particularly at Thackaringa, approximately 20 km to the southwest of the main orebody. The most common epithermal deposits are Cambrian or younger in age and consist essentially of veins of siderite and galena, together with minor quartz, calcite and various sulfides. Some of these veins cut pegmatites, and many are located in faults that transgress the schistosity of retrograde schist zones (Stevens 1986).

The native lead occurs in a vein intersected during underground mining operations in the 1990s by Pasminco on level sixteen (~700 m below surface) of the NBHC mine (Fig. 1). The vein was not recognized as being of interest until its rediscovery in 2004, when the mine was operated by Perilya Limited. The vein is exposed over a total distance of 26 m and attains 7.5 cm in thickness, with a strike of ~040° and dip of 36°E. It is very planar except on the northeastern end, where it intersects and follows a joint (the vein is <1 cm wide at this location) before pinching out. The closest lode to the vein (Fig. 1; Western A Lode) strikes at ~040° and dips 55°W. The host rock of the vein is a weakly retrograded psammite that grades to psammopelite in the footwall. This rock is a very competent, weakly jointed unit, with no obvious shearing or faulting in the immediate vicinity. A weakly bleached zone of alteration rich in white mica is evident to a maximum of four cm on either side of the vein.

The vein is a late-stage feature, cross-cutting local foliation and structures. Near where the vein pinches out to the northeast, it cross-cuts a pegmatite with sharp, well-defined boundaries. Granitic pegmatites composed of quartz, plagioclase and orthoclase together with minor muscovite, biotite and garnet postdate ore formation at Broken Hill and commonly were emplaced within the ore, remobilizing some minerals, particularly galena. These pegmatites also scavenged lead to form a distinctive green (amazonitic), lead-rich orthoclase (Plimer 1976, 1999, Stevenson & Martin 1986).

VEIN MINERALOGY

The mineralogy of the lead-bearing vein varies along the exposed strike. The identity of all species has been confirmed by scanning electron microscopy, energy-dispersive spectrometry and X-ray diffraction. The southwestern end consists almost entirely (~90%, based on visual estimate) of laumontite, with the remainder being biotite and muscovite, together with minor

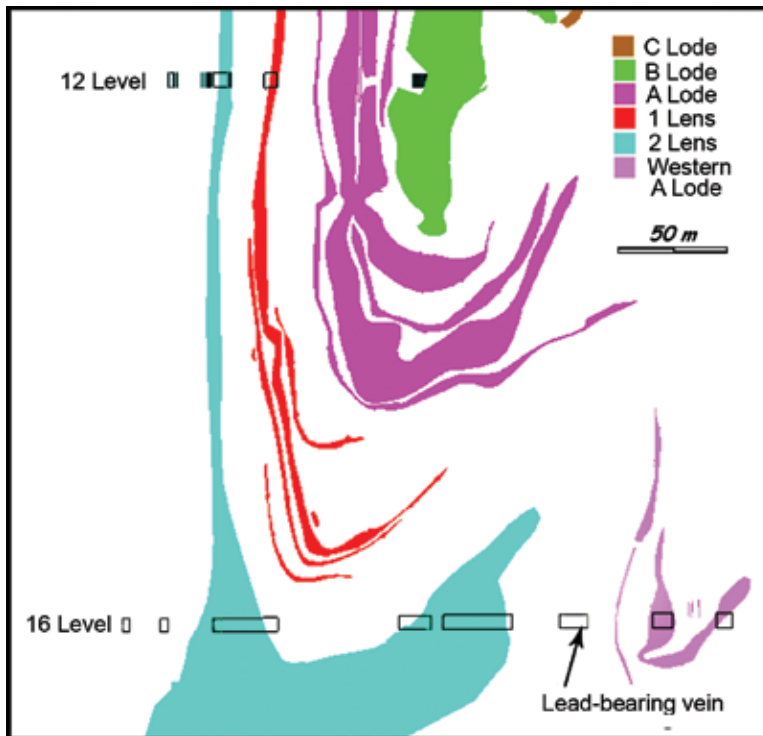


FIG. 1. Cross-section of lower part of Broken Hill orebody at the Perilya southern operations (NBHC) mine showing locations of the 12 and 16 levels and the occurrence of native lead. The 3 lens lode is uneconomic in this region and, if present, would occur on the other side of 2 lens to the native lead.

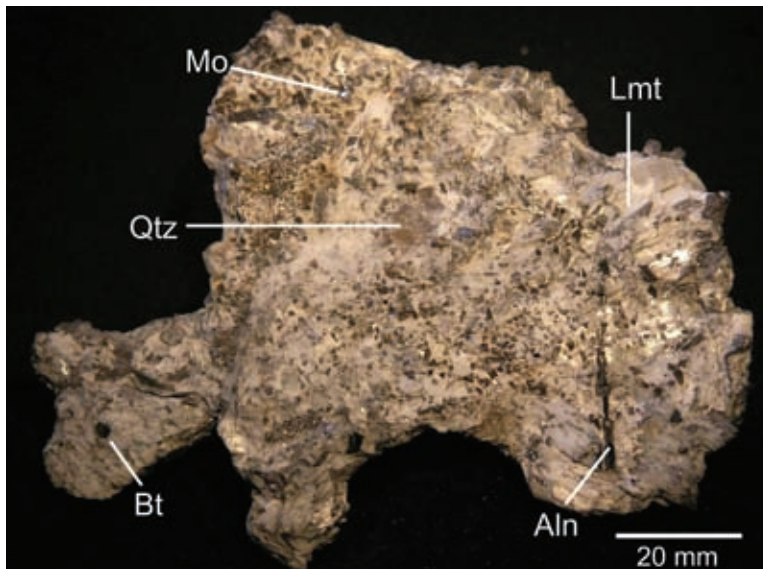


FIG. 2. Sample of lead-bearing vein from Broken Hill showing (Lmt) laumontite, (Qtz) quartz, (Bt) biotite, (Aln) allanite-(Ce), (Ms) muscovite and (Mo) molybdenite.

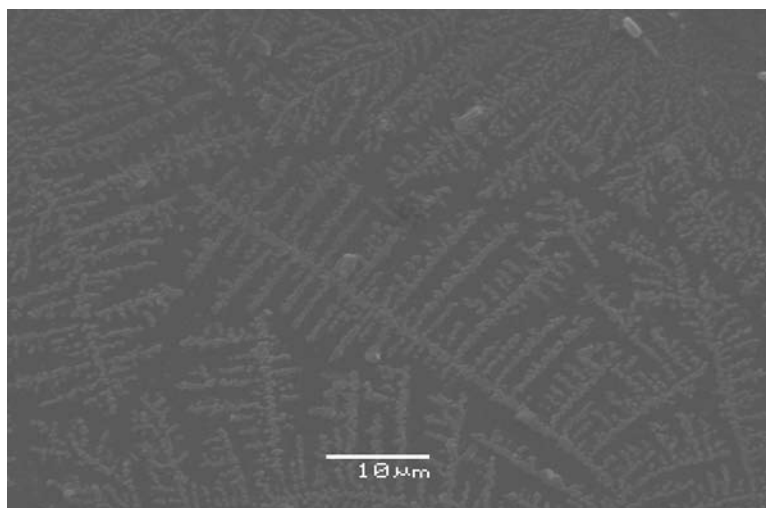


FIG. 3. Skeletal sylvite in muscovite from lead-bearing vein, Broken Hill.

staining by iron oxides and hydroxides. Approximately halfway along the exposure, the vein reaches its widest development (7.5 cm) over a 2 m section and consists of laumontite (60%), quartz (25%), micas (biotite and muscovite; 10%), sulfides (4%), lead (trace), and rare allanite-(Ce). As the northwestern end of the exposure is approached, all minerals except laumontite and quartz (which occur in equal proportions) disappear.

Laumontite is by far the major component of the vein and constitutes >50% in all parts of the exposure. Crystals are white and prismatic (Fig. 2), with a maximum length of ~20 mm, but typically are $15 \times 4 \times 4$ mm in size. Quartz is clear, glassy and occurs as irregular masses up to 6 mm across scattered throughout the laumontite. Biotite is the major mica and occurs as large (up to 40 mm wide), well-formed hexagonal books up to 10 mm thick (Fig. 2). Muscovite is colorless, lustrous and forms near-perfect hexagonal books approximately 1 mm across and up to 4 mm long (Fig. 2). These books are mainly concentrated along the vein margins but, in some cases, surround the native lead. The energy-dispersion spectra for both biotite and muscovite are indicative of Cl-rich species. In addition, skeletal crystals of sylvite are common along the cleavage surfaces of muscovite (Fig. 3).

The sulfides and lead occur in the widest part of the vein. The sulfides comprise irregular, mainly millimetric grains of sphalerite and galena, but one piece of combined massive galena and sphalerite measures 30 mm across. These sulfides are scattered throughout the laumontite, although some grains of galena are encased in quartz. In addition, very rare and very small (<1 mm), irregular blebs of molybdenite have been recognized (Fig. 2). Lead occurs as rare, grey, fresh, irregular,

rounded masses mainly up to 20 mm in maximum dimension, but one piece measures $130 \times 70 \times 20$ mm (Fig. 4).

The compositional purity of the native lead was checked by energy-dispersive X-ray-fluorescence spectrometry of several flat surfaces (approximately 10×10 mm) of native lead samples utilizing a SPECTRO XEPOS instrument. With this technique, one does not produce high-precision analyses, but one can identify which elements are present and their approximate content. In addition to Pb, the spectra indicate the presence of Si, Al, Ca, Cu, Zn and S, reflecting inclusions of laumontite and Cu and Zn sulfides, together with trace amounts of As (100–300 ppm) and Sb (100–500 ppm), which are probably incorporated in the lead.

The only other phase recognized in the lead-bearing vein occurs in one small area as black, single, well-formed, prismatic crystals up to 26 mm in length (Fig. 2). Results of a partial analysis of this phase are presented in Table 1. Comparison of this material with data in Hoshino *et al.* (2006), and mindful of the recommendations of Ercit (2002), we suggest that the phase is allanite-(Ce).

FLUID INCLUSIONS

Methods

Fluid-inclusion microthermometric studies were performed on doubly polished quartz fragments extracted by hand-picking from lightly crushed vein material. Individual samples 70–120 μm thick and 4–8 mm in overall dimension were mounted in a Fluid Inc. USGS-design heating-cooling stage. The

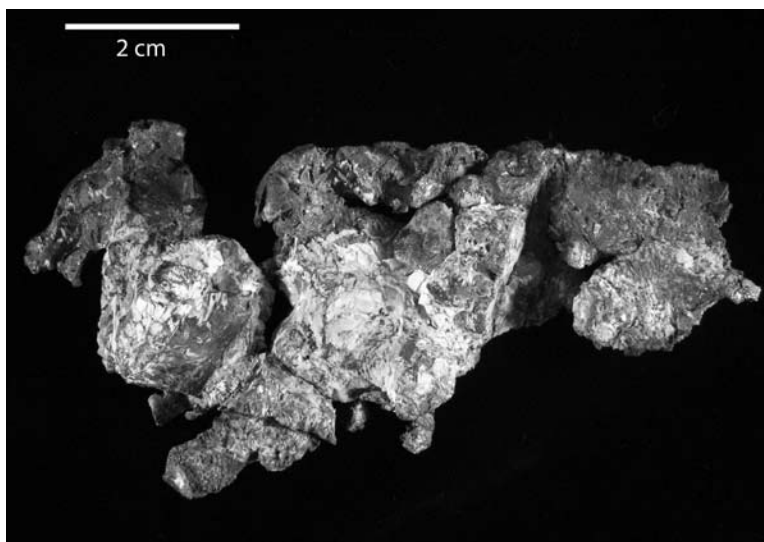


FIG. 4. Native lead from Broken Hill.

thermocouple was calibrated at 0°C using an ice-water bath, and at 374°C (triple point of water) and -56.6°C (freezing point of CO₂) using artificial fluid inclusions. Heating and cooling rates were 5°C per minute overall, but limited to 1–2°C per minute as temperatures of homogenization or final melting of ice were approached. Heating runs on each chip were done before cooling runs; the reproducibility of temperatures of homogenization during heating and ice melting was ±1.0°C.

Results

Three types of fluid inclusions were identified in quartz from the vein. Type 1 consists of irregular to subequant, two-phase (L + V) aqueous inclusions lacking daughter crystals (Fig. 5A). They occur in linear arrays that predate other types of inclusions, but are best interpreted as being secondary on the basis of linear alignments and apparent “necking down” geometries. These inclusions have homogenization temperatures (T_h) in the range 292 to 320°C (Table 2). The liquid phase forms a yellowish “glassy” ice at *ca.* -70°C. Upon warming, mottled crystals of ice become visible at *ca.* -50°C. Final temperatures of ice melting (T_m determined in three fluid inclusions only owing to anomalous freezing behavior) range from -22 to -19°C. These data are consistent with a CaCl₂–NaCl–KCl–H₂O brine with a salinity of *ca.* 19 wt% NaCl eq., calculated using the constants of Brown & Lamb (1989), with the aid of the program FLINCOR. These inclusions most closely resemble the “Type-6” inclusions described at Broken Hill by Wilkins (1977).

TABLE 1. RESULTS OF A PARTIAL ANALYSIS OF ALLANITE-(Ce) FROM THE LEAD-BEARING VEIN, BROKEN HILL

| SiO ₂ | Al ₂ O ₃ | FeO* | CaO | La ₂ O ₃ | Ce ₂ O ₃ | Nd ₂ O ₃ | ThO ₂ | Total |
|------------------|--------------------------------|-------|-------|--------------------------------|--------------------------------|--------------------------------|------------------|-------|
| 32.69 | 20.61 | 10.02 | 13.66 | 4.04 | 6.84 | 2.87 | 3.25 | 93.98 |

FeO*: total Fe expressed as FeO. The data are reported in wt%.

Type-2 fluid inclusions are “packed” with daughter crystals (Fig. 5B), and form linear arrays consistent with a fracture-filling origin. These inclusions contain an aqueous fluid, an aqueous vapor bubble and a suite of daughter crystals that typically include two isotropic euhedral species, a high-birefringence subhedral phase and a high-birefringence anhedral phase. Some of these fluid inclusions also contain a micrometric opaque daughter crystal that did not melt or homogenize after holding the fluid inclusion a few degrees above the homogenization temperature of all other phases. Approximately 20% of the daughter-rich inclusions have a brownish film on the inclusion wall, perhaps representing a high-molecular-weight hydrocarbon phase. This material did not homogenize on heating. The daughter-rich inclusions resemble the “Type-4” inclusions noted at Broken Hill by Wilkins (1977).

Upon cooling from the liquid–vapor homogenization, solid daughter phases reappear as masses of fine, indistinct crystals. Larger daughter crystals reform when the fluid inclusion is held at temperatures slightly below the melting temperature of that phase. Upon cooling, these fluid inclusions form a yellow-amber

“glassy” ice at $<-70^{\circ}\text{C}$. The abundant daughter crystals preclude reliable observation of the final temperatures of ice melting. A typical inclusion containing daughter

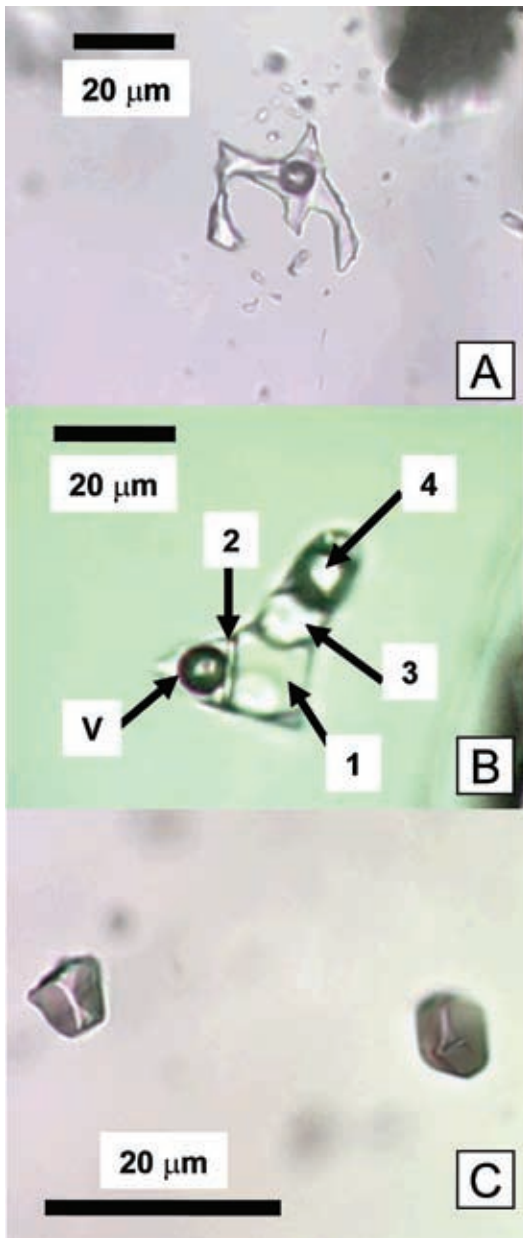


FIG. 5. Fluid inclusions hosted by quartz in native-lead-bearing vein. A. Two-phase (liquid + vapor) aqueous inclusion (P7; $T_h = 309^{\circ}\text{C}$). B. Daughter-crystal-rich inclusion; V: $T_h = 210^{\circ}\text{C}$; Solid 1: $T_m = 110^{\circ}\text{C}$; Solid 2 (partially hidden by vapor bubble): $T_m = 233^{\circ}\text{C}$; Solid 3: $T_m = 255^{\circ}\text{C}$; Solid 4: $T_m > 300^{\circ}\text{C}$. C. Vapor-only fluid inclusions.

crystals and vapor is illustrated in Figure 6. The pattern of behavior of T_h and T_m for the 12 fluid inclusions analyzed are summarized in Table 3 and suggest a salinity >25 wt% NaCl eq. There is a relatively wider range of T_h and T_m , but necking down can be ruled out, as the apparent ratio of solid daughter crystals to fluid is similar among the inclusions examined.

Inclusions of type 3 are vapor-only fluid inclusions. They occur in linear arrays that cross-cut arrays of daughter-rich fluid inclusion. The vapor-only inclusions are dark, negative-crystal forms 5–20 μm in dimension (Fig. 5C). The inclusions contain a single vapor phase that forms two immiscible liquids at *ca.* -70°C when cooled, consistent with the presence of CO_2 . These inclusions resemble the “Type-8” ($\text{CO}_2 + \text{CH}_4$) inclusions of Wilkins (1977).

SEM–EDS examination of breached fluid inclusions in fractured quartz

Centimeter-scale samples of quartz from the vein were lightly crushed and mm-scale fragments were mounted on aluminum stubs using carbon emulsion cement. Samples were gold-coated and imaged using a JEOL–6300 LV scanning electron microscope (SEM). Semiquantitative elemental abundances were determined using an attached PGT Spirit energy-dispersive X-ray spectrometer (EDS). Operating conditions of

TABLE 2. DATA FOR AQUEOUS TWO-PHASE FLUID INCLUSIONS IN QUARTZ FROM THE LEAD-BEARING VEIN, BROKEN HILL

| Inclusion number | T_h ($^{\circ}\text{C}$) | | Inclusion number | T_m ($^{\circ}\text{C}$) | |
|------------------|------------------------------|--------|------------------|------------------------------|--------|
| | liquid+vapor | liquid | | liquid+vapor | liquid |
| P1 | 311 | n.d. | P6 | 301 | n.d. |
| P2 | 320 | n.d. | P7 | 309 | n.d. |
| P3 | 313 | n.d. | P8 | 315 | n.d. |
| P4 | 292 | -22 | P9 | 297 | -19 |
| P5 | 298 | -20 | | | |

n.d.: not determined (see text for discussion).

TABLE 3. DATA FOR DAUGHTER-CRYSTAL-RICH FLUID INCLUSIONS IN QUARTZ FROM THE LEAD-BEARING VEIN, BROKEN HILL

| Inclusion number | T_h ($^{\circ}\text{C}$) | T_m ($^{\circ}\text{C}$) | T_m ($^{\circ}\text{C}$) | T_m ($^{\circ}\text{C}$) | T_m ($^{\circ}\text{C}$) |
|------------------|------------------------------|------------------------------|------------------------------|------------------------------|------------------------------|
| | vapor | solid 1 halite? | solid 2 sylvite? | solid 3 Pb-Cl phase? | solid 4 laumontite? |
| S1 | 215 | 133 | 250 | 254 | 238 |
| S2 | 253 | 114 | 240 | 266 | 305 |
| S3 | 210 | 110 | 233 | 255 | n.d. |
| S4 | 233 | 130 | 241 | n.d. | n.d. |
| S5 | 213 | 129 | 251 | n.d. | n.d. |
| S6 | 239 | 124 | 257 | 232 | 302 |
| S7 | 211 | 116 | 260 | 244 | n.d. |
| S8 | 217 | 117 | 251 | 243 | 270 |
| S9 | 277 | n.d. | n.d. | n.d. | n.d. |
| S10 | 239 | n.d. | n.d. | n.d. | n.d. |
| S11 | 309 | n.d. | n.d. | n.d. | n.d. |
| S12 | 262 | n.d. | n.d. | n.d. | n.d. |

15 kV accelerating voltage and a working distance of ca. 15 mm were maintained.

Breached fluid inclusions with no associated daughter crystals have a surrounding thin accumulation of Ca–K–Cl salts, as identified in EDS spectra. The EDS spectra suggest that Na is a minor constituent of the fluid. Breached daughter-rich fluid inclusions (Fig. 6) show similar accumulations of Ca–K–Cl salts, and partially excavated daughter crystals. The darkened area above the large central inclusion in the secondary electron (SE; Fig. 6) image is K–Cl-rich on the basis of EDS spectra. Similarly, the EDS spectrum of the spot shown in Figure 6 indicates the presence of Ca, K, Cl, Pb and Si, together with Au from the coating of the sample. The small size of the daughter crystals and their close proximity within the breached fluid inclusions limits the precision of EDS spectral determinations; however, clear associations of Pb + Cl in EDS spectra with BSE-bright subhedral crystals (Fig. 7) strongly suggest the presence of a Pb–Cl or Pb–Cl–O mineral as one of the daughter crystals. Similarly, wiry BSE-bright material strongly supports the presence of native lead as a minor daughter phase in the inclusions (Fig. 7). The $SK\alpha$ peak, which would cause asymmetry of the $PbM\alpha$ peak on the EDS spectrum, was not seen, suggesting that S is a minor constituent of the daughter mineral solids. The common occurrence of fissure-hosted lead oxychloride minerals formed from saline aqueous solutions in the Långban deposits, Sweden (Jonsson 2003) suggests that the Broken Hill fluid inclusions may also be Pb oxychloride minerals.

STABLE ISOTOPE DATA

One sample of quartz from the vein was analyzed for oxygen isotopes at the Department of Geological Sciences, University of Wisconsin, stable isotope laboratory using laser fluorination techniques (Spicuzza *et al.* 1998). The $\delta^{18}O_{SMOW}$ of +11.7‰ is typical of quartz in continental crustal rocks. Assuming equilibrium with the hydrothermal fluids at a temperature of ca. 300°C established by T_h of fluid inclusions and laumontite stability, and using the constants of Matsuhisa *et al.* (1979), H_2O in equilibrium with quartz would have had a $\delta^{18}O_{SMOW}$ of 4.8‰. This value is consistent with hydrothermal fluid derived from a crystallizing magma, but it is also consistent with moderately evaporated or evolved seawater, or evolved meteoric water as the mineralizing fluid (Hoefs 1987).

LEAD ISOTOPE DATA

The lead isotopic composition of the native lead sample was determined on a VG ISOMASS 54E solid-source thermal ionization mass spectrometer at the CSIRO Division of Exploration and Mining, Sydney, with a typical precision of $\pm 0.05\%$ (2σ) for

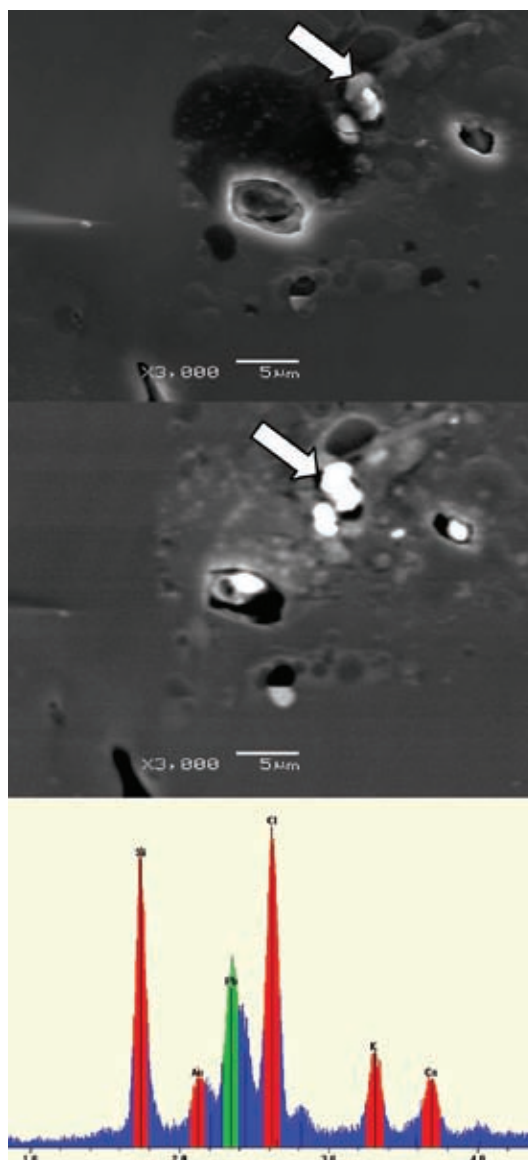


FIG. 6. Breached daughter-crystal-rich fluid inclusions in quartz from native-lead-bearing vein at Broken Hill. Secondary electron (SE) image above; back-scattered electron image (BSE) image below. Energy-dispersion X-ray spectrum (EDS) was acquired with beam centered on BSE bright phase indicated by arrow. Darkened central area above large inclusion (in SE) is (K + Cl)-rich, as indicated by EDS. EDS spectrum illustrated shows Ca, K, Cl, Pb and Au (from coating on sample) and Si peaks. Calcium, K and Cl peaks are likely from laumontite and KCl. Bright phases in BSE are lead-bearing, likely native Pb and Pb–Cl phase.

the $^{207}\text{Pb}/^{204}\text{Pb}$ ratio. Data have been normalized to the accepted values of international standard NBS981 by applying a correction factor of +0.08% per atomic mass unit. The $^{206}\text{Pb}/^{204}\text{Pb}$, $^{207}\text{Pb}/^{204}\text{Pb}$ and $^{208}\text{Pb}/^{204}\text{Pb}$ values are 16.347, 15.484 and 35.934, respectively, and are plotted on Figure 8, together with published reference-data from the Broken Hill area. Galena and associated lead-rich amazonitic orthoclase from the Broken Hill orebody plot as a very tight cluster with a characteristic $^{206}\text{Pb}/^{204}\text{Pb}$ value of ~ 16 (Fig. 8; Stevenson & Martin 1986, Parr *et al.* 2004, de Caritat *et al.* 2005). In contrast to the galena from the Broken Hill orebody, galena from Cambrian epithermal veins in the region (*e.g.*, at Thackaringa, *ca.* 25 km from the orebody) have higher $^{206}\text{Pb}/^{204}\text{Pb}$ values with a much broader spread. The Pb isotopic composition of the native lead sample is clearly removed from the Broken Hill orebody cluster and plots at the low $^{206}\text{Pb}/^{204}\text{Pb}$ end of the spectrum of values for the younger, epithermal galena (Fig. 8).

The pegmatites containing the amazonitic orthoclase postdate the orebody and originated by *in situ* melting of quartzofeldspathic assemblages during the Olarian Orogeny at *ca.* 1600 Ma (Plimer 2006). The close similarity between the Pb isotopic composition of the amazonitic orthoclase and galena strongly suggests that the Pb in the orthoclase originated from the Broken Hill orebody (Stevenson & Martin 1986). In contrast, the isotopic composition of the native lead suggests that it is part of the younger generation responsible for the epithermal deposits, but that it may have had input from the Broken Hill orebody.

DISCUSSION

Previous discoveries of native lead from Broken Hill have been attributed to an anthropogenic origin, with formation from either mine fires (Birch 1999) or mine explosions (Ian Plimer, pers. commun., 2005). The fires in NBHC affected levels eight and nine in the mine, which are >350 m vertically above the lead-bearing vein, and ~ 650 m away horizontally; *i.e.*, a minimum separation of >750 m, which is too far removed for the fires to have had any input to the formation of native lead. Explosions associated with mining some high-grade lead lodes at Broken Hill produce flowage of galena into fractures and may result in the formation of elemental lead as a crenulated smear on exposed, broken rock-faces, and along both natural and explosion-induced joints (Ian Plimer, pers. commun., 2005). The occurrence of the native lead as discrete masses completely enclosed in laumontite within the vein rules out any contribution from mine explosions.

Laumontite is not a common mineral at Broken Hill (Birch 1999). It occurs mainly as joint infill, usually ~ 1 mm and rarely >1 cm thick, particularly in the lower parts of the mines and in cores from deeper drill-holes. The presence of abundant laumontite in the lead-bearing

vein provides several constraints for the formation of native lead. Particularly relevant for understanding the conditions attending its genesis are recent studies on zeolite development in active geothermal systems, where calcium aluminosilicates such as laumontite form in a distinct sequence reflecting increasing temperature. Studies of the Wairakai (New Zealand) geothermal field by Steiner (1977) and the Reydarfjördur (Iceland) geothermal field by Liou *et al.* (1987) suggest that the maximum temperature for laumontite stability is 230°C. Frey *et al.* (1991) have constrained the stability field for laumontite in metabasalts to 180–270°C and 1–3 kbar. Calculations based on thermodynamic data for the system $\text{Na}_2\text{O}-\text{CaO}-\text{Al}_2\text{O}_3-\text{SiO}_2-\text{H}_2\text{O}$ and $\text{P}(\text{H}_2\text{O}) = \text{P}_{\text{total}}$ indicate that the lower and upper limits of stability of laumontite are 160–185°C and 235–270°C, respectively, at low pressures (1–2 kbar; Mihalynuk & Ghent 1996). The theoretical maximum temperature for laumontite stability is consistent with the observed occurrences in geothermal systems, but the calculated minimum temperature for laumontite formation is considerably higher than observed temperatures. For example, laumontite has been observed to form under near-surface conditions at temperatures of <50°C (Boles & Coombs 1977, Wopfner *et al.* 1991, Jove & Hacker 1997). These observations suggest that laumontite is stable from surface temperatures up to a maximum of *ca.* 270°C. In addition to the temperature, however, zeolite formation is strongly dependent on other factors, including $\text{P}(\text{H}_2\text{O})$, $\text{P}(\text{CO}_2)$ and fluid chemistry. Recent studies by Wilkinson *et al.* (2001) indicate that laumontite stability is favored by both high pH and low $\text{P}(\text{CO}_2)$. The other mineral present in the vein that has implications for the conditions of formation of the native lead is allanite-(Ce), which has a minimum temperature for formation of 200–250°C (Bird *et al.* 1984, Cho *et al.* 1986, Liou *et al.* 1985, Reyes 1990), thereby providing a lower limit for the temperature of the fluids.

Wilkins (1977) documented the presence of 10 types of fluid inclusions in Broken Hill rocks. The three types of inclusions identified in the current study most strongly resemble Type 6 (aqueous inclusions lacking daughter crystals), Type 4 (daughter-crystal-rich inclusions) and Type 8 ($\text{CH}_4 + \text{CO}_2$ inclusions). Our results are limited to quartz within a vein that is clearly a late hydrothermal feature that cross-cuts earlier structures, and therefore the fluid-inclusion assemblage is less complex than that documented by Wilkins (1977).

Quartz and laumontite are paragenetically coeval within the vein system, an inference based upon the intimate intergrowth of the two phases. The relatively high salinity of the fluid in the aqueous inclusions (*ca.* 19 wt% NaCl eq., based on final temperatures of ice melting), and the presence of K–Ca–Cl salts in breached inclusions, are consistent with the Cl-rich nature of accompanying muscovite and biotite, and the common presence of skeletal crystals of sylvite along cleavage

surfaces of muscovite. The homogenization temperature of *ca.* 300°C for the aqueous, daughter-free inclusions is slightly higher than the maximum temperature of formation suggested by the occurrence of laumontite in the vein, but the combined fluid-inclusion and mineral-stability data are compatible with a temperature of 270–300°C.

The daughter-crystal-rich fluid inclusions may represent fluids trapped during the latter stages of active hydrothermal mineralization, with the abundant solids resulting from precipitation from the cooling fluids along narrow fractures in primary quartz. The variable temperatures of vapor homogenization observed are consistent with this model, but the relatively constant liquid:solid ratios in these inclusions may support their origin from a later, much higher-salinity fluid, perhaps approaching 50 wt% NaCl eq., on the basis of qualitative estimates of the solid:liquid ratio in the inclusions at 20°C. If the vein was emplaced within country rock that initially lacked hydrous silicate minerals, retrograde hydration reactions within the wallrock of the vein could have raised the salinity of the remaining hydrothermal fluids, leaving highly concentrated late brine (Yardley & Graham 2002) available to form the daughter-crystal-rich fluid inclusions.

The presence of native Pb and a Pb–Cl or Pb–Cl–O phase within the daughter-rich inclusions suggests that the later fluids carried high concentrations of dissolved lead, likely complexed with chloride. These fluids were presumably similar to the late-stage, low-temperature (<325°C) fluids that deposited a variety of rare Pb oxychloride species together with native lead as fissure and vein infillings in the Långban Mn–Fe deposits of Sweden (Jonsson 2003). The apparent absence of sulfide minerals within the daughter-rich inclusions, in contrast to brine-sulfide trails described by Williams *et al.* (2005) for Broken Hill galena-bearing assemblages, suggests that the fluids that deposited the laumontite vein were oxidized. The proposal for the involvement of brines in the formation of Broken Hill minerals is certainly not new. The fluid that deposited the famous Pb–Zn–Ag lodes has been interpreted as being highly saline as a result of circulation through evaporate-rich strata that underlie the ores (Plimer 1994, Slack *et al.* 1993).

The Långban Mn–Fe ore deposit is famous not only as the type locality for more than 60 minerals, but also for the large number (approximately 270) of mineral species recognized (Nysten *et al.* 2000). These species developed during several episodes of mineral formation, with the youngest producing an assemblage of late-stage, rare and exotic species in a series of fissures that cross-cut the other rocks in the deposit. These fissures range in dimensions from microscopic to veins tens of cm across, and the included minerals occur as fillings, thin coatings on fissure surfaces, and as well-developed crystals. Native lead occurs within fissures as individual crystals up to 6 cm across and as masses of up to 51 kg

(Nysten *et al.* 2000). Fluid inclusion, and carbon and oxygen isotopic data indicate that these late-stage minerals formed from low-temperature (70–180°C), moderately to highly saline aqueous fluids (*i.e.*, brines), in a near-surface environment (Jonsson & Boyce 2002). Reactions between the moderately to highly saline aqueous fluids and the abundant Mn-bearing carbonate host-rocks at Långban led to a dramatic increase in pH of the fluid and a concomitant release of sulfate and Mn²⁺. Transition from pervasive flow at depth to channelized flow in fissures associated with a shallow, brittle tectonic environment produced a drop in pressure, boiling of the fluid, and precipitation of the late-stage minerals. On the basis of sulfur isotopic data, Bostrom (1996) estimated a temperature of *ca.* 325°C for the formation of native lead, analogous to the temperature proposed for Broken Hill hydrothermal system that precipitated the lead-bearing vein.

The petroleum fields of Mississippi and north-western Europe, and a geothermal field in Turkmenistan (former Soviet Union) provide modern examples of precipitation of elemental lead, galena and barite from brines. In these areas, these minerals commonly occur as scale on the steel tubing for well and surface installations, but in northwestern Europe, lead also forms precipitates up to several cm in size and 1.5 kg in mass in well tubing at perforation depth (Schmidt 1998). On exiting the buffered environment of the petroleum reservoir and entering the well tube, the fluid undergoes a dramatic change in physicochemical conditions so that Fe²⁺ is dissolved from the steel well tubing and lead is precipitated (Schmidt 1998). The brines that precipitate lead in the Mississippi petroleum fields are K-rich and at temperatures of 109–135°C (Carpenter *et al.* 1974). Precipitation of lead scale in well tubing in these petroleum fields is restricted to those wells that use pumps for the production of fluids (Carpenter *et al.* 1974). Similarly, Schmidt (1998) concluded that precipitation of lead scale in the European petroleum fields seems to be related to the turbulence and pressure differences or intense corrosion associated with pumps. These observations suggest that formation of lead masses near well-tube perforations may be the result of change from pervasive flow of fluid through the reservoir to channelized flow in the wells.

At Broken Hill, the obvious potential source for the lead that ultimately precipitated in the vein is the massive sulfide bodies for which the region is famous. The ²⁰⁷Pb/²⁰⁴Pb value for the native lead (16.347), however, is significantly higher than the characteristic value (*ca.* 16.0) for the Broken Hill lode and overlaps with the lower end of the array defined by Cambrian epithermal galena deposits in the region. The Pb isotopic data suggest that the native lead and the Cambrian epithermal deposits had a common source, but that the native lead may have been affected by more recent supergene processes that involved mixing with

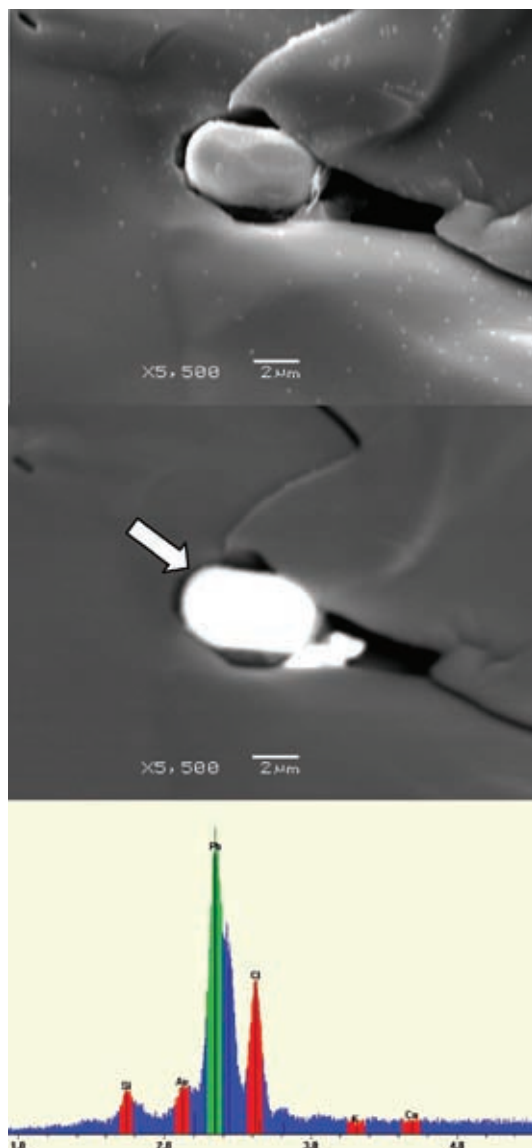


FIG. 7. Breached fluid-inclusions in quartz from lead-bearing vein, Broken Hill. Arrows indicate locations of spot EDS analyses. Lead-bearing phases in breached fluid-inclusion in quartz. SE above, BSE below. Ovate crystal is likely Pb–Cl phase; wiry phase to right of crystal (as seen in SE image) is likely native Pb. Bright blocky phase below wiry phase also is Pb-bearing. Electron beam was centered on the ovate crystal during spectrum acquisition. Note the symmetry of the $PbM\alpha$ X-ray peak, and the presence of a well-defined $PbM\beta$ peak, indicating that S is minor or absent.

lead from the Broken Hill lode to produce the lower $^{207}Pb/^{204}Pb$ value. A similar lead isotope pattern is present in epithermal galena–calcite veins located near the Proterozoic Balmat Zn–Pb deposit in New York State (Ayuso *et al.* 1989). In that system, relatively more radiogenic lead was derived from sandstones that overlie the Proterozoic deposits, with epithermal mineralization occurring in the Late Paleozoic. The lead isotope signature of the epithermal galena is the result of mixing of the lead from two reservoirs.

Harrison & McDougall (1981) identified a thermal pulse associated with the Delamerian Orogeny at *ca.* 520 Ma, when temperatures rose to *ca.* 350°C in some parts of the Broken Hill region. The fluids associated with the retrograde metamorphism accompanying this thermal pulse also were responsible for the formation of the epithermal deposits of galena in the region (Yibao *et al.* 1987) and, by inference, the lead-bearing vein.

The presence of possible films of residual hydrocarbon in fluid inclusions and the presence of likely CO_2 plus CH_4 in fluid inclusions in the Broken Hill lead-bearing vein suggest that the hydrothermal fluids may have originated in sedimentary or metamorphic rocks containing organic material. Irrespective of the source, the lead then remained in solution until the physicochemical conditions changed sufficiently that it precipitated.

On the basis of the fluid inclusions, the stability of the mineral assemblage, and by analogy with the lead-bearing, late-stage fissures at Långban, and the petroleum and geothermal fields, the Broken Hill native lead and associated minerals are interpreted to have formed by precipitation from brines in a near-surface, low-pressure environment. Where the brines flowed pervasively at deeper, higher-pressure levels in the Broken Hill system and the pH was near neutral, the lead remained in solution. Near-surface fracturing changed conditions to a channelized flow regime and lower pressure. The occurrence of the native lead in the widest part of the vein may reflect the lower-pressure regime associated with widening of the fissure. Reaction between fluids and enclosing Mn-bearing rocks raised the pH of the fluids and lowered the $P(CO_2)$ to precipitate the native lead and laumontite.

The temperature of mineralization indicated by mineral stability and fluid-inclusion data is near the melting point of native lead (327°C), raising the possibility that the lead was in a molten state when emplaced. It has been proposed (Frost *et al.* 2002, 2005) that sulfide ores in the main Broken Hill Zn–Pb–Ag system were mobilized and locally emplaced as melts during regional metamorphism at temperatures greater than 550°C. The mineral assemblages and textural attributes of the native-lead-bearing vein, however, argue strongly for a hydrothermal origin. The fluids responsible for vein mineralization may represent distal fractionates from sulfide melts, as described by Williams *et al.* (2005). However, the sulfide-poor nature

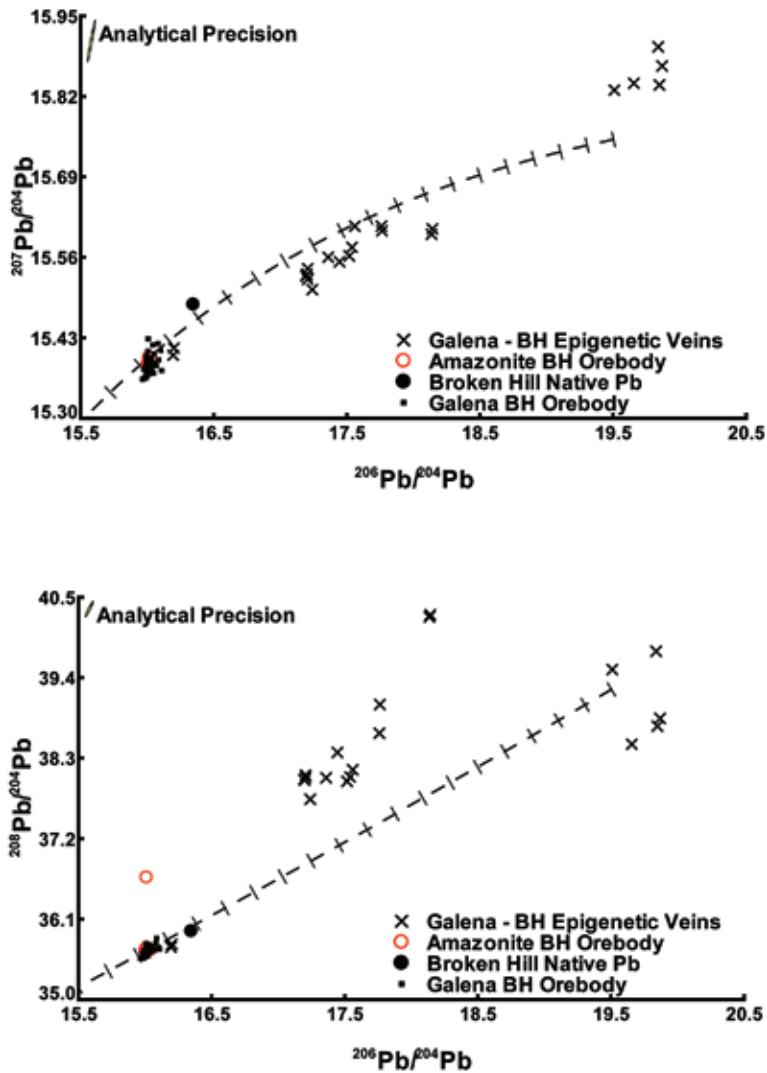


FIG. 8. Plots of $^{207}\text{Pb}/^{204}\text{Pb}$ and $^{208}\text{Pb}/^{204}\text{Pb}$ versus $^{206}\text{Pb}/^{204}\text{Pb}$ for native lead from Broken Hill. Data for galena and amazonitic orthoclase from the Broken Hill orebody, together with data for galena from epithermal veins in the region, are shown for comparison. Reference data from Stevenson & Martin (1986) and de Caritat *et al.* (2005). Growth curve from Stacey & Kramers (1975).

of the vein minerals and daughter crystals in fluid inclusions requires an oxidizing, near-neutral-pH fluid, thus demanding considerable alteration of the composition of a sulfide-melt fractionate.

ACKNOWLEDGEMENTS

The authors gratefully acknowledge Ian Plimer for his discussions on the origin of Broken Hill minerals.

The constructive reviews of Robert F. Martin, Paul Spry, Ross A. Both, and an anonymous referee are very much appreciated. Paul Millsted and Graham Carr carried out the analysis of the allanite-(Ce) and isotopic analysis of the native lead, respectively. PFC acknowledges support from the GeoQuEST Research Centre at the University of Wollongong.

REFERENCES

- AYUSO, R.A., FOLEY, N.K. & BROWN, C.E. (1987): Source of lead and mineralizing brines for Rossie-type Pb–Zn veins in the Frontenac axis area, New York. *Econ. Geol.* **82**, 489–496.
- BIRCH, W.D., ed. (1999): *Minerals of Broken Hill* (2nd edition). Broken Hill City Council, Broken Hill, Australia, and Museum Victoria, Melbourne, Australia.
- BIRCH, W.D., CHAPMAN, A. & PECOVER, S.R. (1982): The Minerals. In *Minerals of Broken Hill* (H.K. Worner, R.W. Mitchell, eds.). Australian Mining and Smelting Limited, Melbourne, Australia (68–195).
- BIRD, D.K., SCHIFFMAN, P., ELDERS, W.A., WILLIAMS, A.E. & MCDOWELL, S.D. (1984): Calc-silicate mineralization in active geothermal systems. *Econ. Geol.* **79**, 671–695.
- BOLES, J.R. & COOMBS, D.S. (1977): Zeolite-facies alteration of sandstones in the Southland syncline, New Zealand. *Am. J. Sci.* **277**, 982–1012.
- BOSTROM, K. (1996): The temperature of formation of the native lead – pyrochroite veins and related associations in Långban. *Geol. Soc. Sweden, GFF* **118**, A50.
- BROWN, P.E. & LAMB, W.M. (1989): P–V–T properties of fluids in the system $H_2O \pm CO_2 \pm NaCl$: new graphical presentations and implications for fluid inclusion studies. *Geochim. Cosmochim. Acta* **53**, 1209–1221.
- CARPENTER, A.B., TROUT, M.L. & PICKETT, E.E. (1974): Preliminary report on the origin and chemical evolution of lead- and zinc-rich oil field brines in central Mississippi. *Econ. Geol.* **69**, 1191–1206.
- CHO, MOONSUP, LIOU, J.G. & MARUYAMA, S. (1986): Transition from the zeolite to prehnite–pumpellyite facies in the Karmutsen metabasites, Vancouver Island, British Columbia. *J. Petrol.* **27**, 467–494.
- DE CARITAT, P., KIRSTE, D., CARR, G. & MCCULLOCK, M. (2005): Groundwater in the Broken Hill region, Australia: recognising interaction with bedrock and mineralisation using S, Sr and Pb isotopes. *Applied Geochem.* **20**, 767–787.
- DUNN, P.J. (1995): *Franklin and Sterling Hill, New Jersey: the World's Most Magnificent Mineral Deposits*. Department of Mineral Science, Smithsonian Institution, Washington, D.C.
- ERCIT, T.S. (2002): The mess that is “allanite”. *Can. Mineral.* **40**, 1411–1419.
- FREY, M., DE CAPITANI, C. & LIOU, J.G. (1991): A new petrogenetic grid for low-grade metabasites. *J. Metam. Geol.* **9**, 497–509.
- FROST, R.B., MAVROGENES, J.A. & TOMKINS, A.G. (2002): Partial melting of sulfide ore deposits during medium and high-grade metamorphism. *Can. Mineral.* **40**, 1–18.
- FROST, R.B., SWAPP, S.M. & GREGORY, R.W. (2005): Prolonged existence of a sulfide melt in the Broken Hill orebody, New South Wales, Australia. *Can. Mineral.* **43**, 479–493.
- HARRISON, T.M. & MCDUGALL, I. (1981): Excess ^{40}Ar in metamorphic rocks from Broken Hill, New South Wales: implications for $^{40}Ar/^{39}Ar$ age spectra and the thermal history of the region. *Earth Planet. Sci. Lett.* **55**, 123–149.
- HOEFS, J. (1987): *Stable Isotope Geochemistry* (3rd edition). Springer-Verlag, Berlin, Germany.
- HOSHINO, M., KIMATA, M., SHIMIZU, M., NISHIDA, N. & FUJIWARA, T. (2006): Allanite-(Ce) in granitic rocks from Japan: genetic implications of patterns of REE and Mn enrichment. *Can. Mineral.* **44**, 45–62.
- JAXEL, R. & GELAUE, P. (1986): New mineral occurrences from the Laurium (Greece) slags. *Mineral. Rec.* **17**, 183–190.
- JONSSON, E. (2003): Mineralogy and paragenesis of Pb oxychlorides in Långban-type deposits, Bergslagen, Sweden. *Geol. Soc. Sweden, GFF* **125**, 87–98.
- JONSSON, E. & BOYCE, A.J. (2002): Carbon and oxygen isotopes as indicators of hydrothermal processes in the Långban area, Bergslagen. *Geol. Soc. Sweden, GFF* **124**, 234–235 (abstr.).
- JOVE, C. & HACKER, B.R. (1997): Experimental investigation of laumontite \rightarrow wairakite + H_2O : a model diagenetic reaction. *Am. Mineral.* **82**, 781–789.
- LIU, G.L., MARUYAMA, S. & CHO, MOONSUP (1987): Very low-grade metamorphism of volcanic and volcanoclastic rocks – mineral assemblages and mineral facies. In *Low Temperature Metamorphism* (M. Frey, ed.). Blackie, Glasgow, U.K. (59–113).
- LIU, J.G., SEKI, Y., GUILLEMETTE, R. & SAKAI, H. (1985): Compositions and paragenesis of secondary minerals in the Onikobe geothermal system, Japan. *Chem. Geol.* **49**, 1–20.
- MATSUHIRA, Y., GOLDSMITH, J.R. & CLAYTON, R.N. (1979): Oxygen isotopic fractionation in the systems quartz – albite – anorthite – water. *Geochim. Cosmochim. Acta* **43**, 1131–1140.
- MIHALYNUK, M.G. & GHENT, E.D. (1996): Regional depth-controlled hydrothermal metamorphism in the Zymoetz River area, British Columbia. *Can. J. Earth Sci.* **33**, 1169–1184.
- NYSTEN, P., HOLTSTAM, D. & JONSSON, E. (2000): The Långban minerals. In *Långban: the Mines, their Minerals, Geology and Explorers* (D. Holtstam & J. Langhof, eds.). Raster Forlag and the Swedish Museum of Natural History, Stockholm, Sweden (89–183).
- PARR, J.M., STEVENS, P.J., CARR, G.R. & PAGE, R.W. (2004): Subseafloor origin for Broken Hill Pb–Zn–Ag mineralization, New South Wales, Australia. *Geology* **32**, 589–592.

- PLIMER, I.R. (1976): A plumbian feldspar pegmatite associated with the Broken Hill orebodies, Australia. *Neues Jahrb. Mineral., Monatsh.*, 272-288.
- PLIMER, I.R. (1994): Strata-bound scheelite in meta-evaporites, Broken Hill, Australia. *Econ. Geol.* **89**, 423-437.
- PLIMER, I.R. (1999): The Making of the Minerals. In Minerals of Broken Hill (W.D. Birch, ed.; 2nd edition). Broken Hill City Council, Broken Hill, Australia, and Museum Victoria, Melbourne, Australia (70-87).
- PLIMER, I.R. (2006): Manganian garnet rocks associated with the Broken Hill Pb-Zn-Ag orebody, Australia. *Mineral. Petrol.* **88**, 443-478.
- REYES, A.G. (1990): Petrology of Philippine geothermal systems and the application of alteration mineralogy to their assessment. *J. Volcan. Geotherm. Res.* **43**, 279-309.
- SCHMIDT, A.P. (1998): Lead precipitates from natural gas production installations. *J. Geochem. Explor.* **62**, 193-200.
- SLACK, J.F., PALMER, M.R., STEVENS, B.P.J. & BARNES, R.G. (1993): Origin and significance of tourmaline-rich rocks in the Broken Hill district, Australia. *Econ. Geol.* **88**, 505-541.
- SPICUZZA, M.J., VALLEY, J.W., KOHN, M.J., GIRAND, J.P. & FOULLAC, A.M. (1998): The rapid heating, defocused beam technique: a CO₂-laser-based method for highly precise and accurate determination of $\delta^{18}\text{O}$ values of quartz. *Chem. Geol.* **144**, 195-203.
- STACEY, J.S. & KRAMERS, J.D. (1975): Approximation of terrestrial lead isotopic evolution by a two stage model. *Earth Planet. Sci. Lett.* **26**, 207-221.
- STEINER, A. (1977): The Wairakei geothermal area, North Island, New Zealand. *N.Z. Geol. Surv. Bull.* **90**, 136.
- STEVENS, B.P.J. (1986): Post-depositional history of the Willyama Supergroup in the Broken Hill Block, NSW. *Aust. J. Earth Sci.* **33**, 73-98.
- STEVENS, B. (1999): The geology of Broken Hill. In Minerals of Broken Hill (W.D. Birch, ed.; 2nd edition). Broken Hill City Council, Broken Hill, Australia, and Museum Victoria, Melbourne, Australia (59-69).
- STEVENSON, R.K. & MARTIN, R.F. (1986): Implications of the presence of amazonite in the Broken Hill and Geco metamorphosed sulfide deposits. *Can. Mineral.* **24**, 729-745.
- WILKINS, R.W.T. (1977): Fluid inclusion assemblages of the stratiform Broken Hill deposit. *Science* **198**, 185-187.
- WILKINSON, M., MILLIKEN, K.L. & HASZELDINE, R.S. (2001): Systematic destruction of K-feldspar in deeply buried rift and passive margin sandstones. *J. Geol. Soc. London* **158**, 675-683.
- WILLIAMS, P.J., DONG, G., ULLRICH, T., RYAN, C. & MERNAGH, T. (2005): Lead- and zinc-rich fluid inclusions in Broken-Hill type deposits: fractionates from sulfide-rich melts or consequences of exotic fluid infiltration? In Mineral Deposit Research: Meeting the Global Challenge (J. Mao, J. & F. P. Bierlein, eds.). Springer, Berlin, Germany (861-864).
- WILLIS, I.L., BROWN, R.E., STROUD, W.J. & STEVENS, B.P.J. (1983): The Early Proterozoic Willyama Supergroup: stratigraphy and interpretation of high- to low-grade metamorphic rocks in the Broken Hill Block, New South Wales. *J. Geol. Soc. Aust.* **30**, 195-224.
- WILSON, C.J.L. & POWELL, R. (2001): Strain localization and high-grade metamorphism at Broken Hill, Australia: a review from the Southern Cross area. *Tectonophysics* **335**, 193-210.
- WOPFNER, H., MARKWORT, S. & SEMKIWA, P.M. (1991): Early diagenetic laumontite in the lower Triassic Manda Beds of the Ruhuhu Basin, southern Tanzania. *J. Sed. Petrol.* **61**, 65-72.
- YARDLEY, B.W.D. & GRAHAM, J.T. (2002): The origins of salinity in metamorphic fluids. *Geofluids* **2**, 249-256.
- YIBAO, D., BOTH, R.A., BARNES, R.G. & SUN, S.S. (1987): Regional stable isotope and fluid inclusion study in the Broken Hill Block, New South Wales, Australia. *Trans. Inst. Mining Metall.* **96**, B15-B30.

Received August 19, 2006, revised manuscript accepted October 6, 2007.

